Three-Dimensional Assessment of Left Ventricular Systolic Strain in Patients With Type 2 Diabetes Mellitus, Diastolic Dysfunction, and Normal Ejection Fraction

Carissa G. Fonseca, BTech, Ajith M. Dissanayake, Robert N. Doughty, Gillian A. Whalley, MHSc, Greg D. Gamble, MSc, Brett R. Cowan, BE, MBChB, Christopher J. Occleshaw, and Alistair A. Young, PhD

Left ventricular (LV) diastolic dysfunction often occurs in patients with type 2 diabetes mellitus (DM) independent of atherosclerotic coronary artery disease, myocardial ischemia, and regional wall motion anomalies. Limited information exists on LV myocardial tissue strain in this patient group. We measured 3-dimensional (3-D) parameters of LV systolic and diastolic functions in 28 patients who had type 2 DM (age 33 to 70 years), standard echocardiographic evidence of LV diastolic dysfunction, and normal LV ejection fraction, and 31 normal control subjects (age 19 to 74 years) who had no evidence of cardiac disease, with multislice cine anatomic and tagged magnetic resonance imaging. Three-dimensional analysis of the resulting images showed that peak systolic mitral valve plane displacement was 12% smaller ($p = 0.040$) and peak diastolic mitral valve plane velocity was 21% lower ($p = 0.008$) in patients who had DM than in normal controls. Peak systolic circumferential and longitudinal strains and principal 3-D shortening strain were 14%, 22%, and 10% smaller, respectively, in the DM group ($p < 0.001$ for each). Peak diastolic rate of relaxation of circumferential and longitudinal strains and principal 3-D shortening strain were 35%, 32%, and 33% lower, respectively, in the DM group ($p < 0.001$ for each). Thus, LV systolic circumferential, longitudinal and 3-D principal strains, and diastolic strain rates are impaired in patients who have type 2 DM, LV diastolic dysfunction, and normal LV ejection fraction.

(Am J Cardiol 2004;94:1391–1395)

This study assessed systolic and diastolic 3-dimensional (3-D) myocardial functions in patients who had type 2 diabetes mellitus (DM) and were identified by echocardiographic criteria as having a normal ejection fraction and diastolic dysfunction. We hypothesized that systolic and diastolic 3-D strain parameters derived with magnetic resonance imaging (MRI), including circumferential, longitudinal, and torsional components of the deformation (and the 3-D principal strain, which is a combination of these components), would be depressed in these patients. In addition, the motion of the mitral valve annulus plane was tracked in 3 dimensions. Because mitral valve plane displacement and velocity are commonly estimated in tissue Doppler imaging and other echocardiographic examinations and are believed to be sensitive indicators of systolic and diastolic functions,[1,2] we hypothesized that MRI-derived 3-D mitral valve plane motion would also be depressed in systole and diastole.

From the Departments of Anatomy With Radiology and Medicine, Faculty of Medical and Health Sciences, University of Auckland; Middlemore Hospital, South Auckland Health; and the Department of Cardiology, Auckland City Hospital, Auckland, New Zealand. This work was supported in part by a grant from the Health Research Council of New Zealand, Auckland, New Zealand. Ms Fonseca and Ms Whalley are funded by postgraduate scholarships from the National Heart Foundation of New Zealand, Auckland, New Zealand. Manuscript received April 13, 2004; revised manuscript received and accepted July 2, 2004.

Address for reprints: Alistair A. Young, Department of Anatomy With Radiology, Faculty of Medical and Health Sciences, University of Auckland, Private Bag 92019, Auckland, New Zealand. E-mail: a.young@auckland.ac.nz.

METHODS

Subjects: Written informed consent was obtained from all subjects, and the institutional ethics committee approved the research protocol. This investigation conformed with the principles outlined in the Declaration of Helsinki.[3] Patients were eligible for inclusion if they had type 2 DM, hemoglobin A1c >7%, evidence of diastolic dysfunction with normal systolic function (cardiac ejection fraction ≥45% and no regional wall motion anomalies), normal electrocardiogram (sinus rhythm, normal PR interval, normal T-wave and QRS morphologies, and an isoelectric ST segment), evidence of diabetic retinopathy, and/or evidence of diabetic nephropathy (urine albumin >300 mg/L and serum creatinine >150 μmol/L). Patients were ineligible if they were pregnant or morbidly obese (body mass index ≥45 kg/m^2), had evidence of autonomic neuropathy, or presented standard contraindications to MRI. Subjects were included in the control group only if their clinical history and examination, transthoracic echocardiogram, and 12-lead electrocardiogram showed no evidence of preexisting cardiac disease or other significant coexisting illness. Exclusion criteria included a history of hypertension, diabetes, ischemic or valvular heart disease, regular use of medication for cardiovascular illness, or a seated blood pressure >160/90 mm Hg. On the 12-lead

0002-9149/04/$–see front matter
doi:10.1016/j.amjcard.2004.07.143

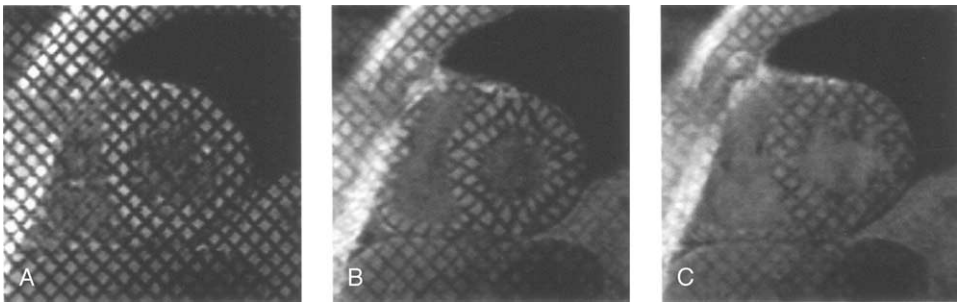

FIGURE 1. Short-axis tagged magnetic resonance images at the mid-ventricular level for a typical patient with type 2 DM show good tag persistence throughout the cardiac cycle at *(A)* end-diastole, *(B)* end-systole, and *(C)* late diastole.

electrocardiogram, atrial fibrillation, bundle branch block, pathologic Q waves, left ventricular (LV) hypertrophy, or changes consistent with myocardial ischemia resulted in exclusion, as did any significant valvular abnormality, impaired systolic LV function, or LV hypertrophy on the transthoracic echocardiogram.

Echocardiography: All echocardiographic examinations were performed with an ATL HDI 5000 echocardiograph (Bothell, Washington). Images were obtained by a research cardiac sonographer according to a standard protocol, recorded onto videotape, and analyzed off-line. For each parameter, 3 measurements were taken and an average value was recorded. In the apical 4-chamber view, a 5-mm pulse-wave Doppler sample volume was placed distally to the mitral annulus, between the mitral leaflets, and measurements were made at the end of the expiratory phase of normal respiration, with the interrogation beam aligned with mitral flow.[4] Peak early transmitral inflow velocity, peak transmitral flow velocity in late diastole, the ratio of early to late peak transmitral flow velocity, and the early filling deceleration time were determined from these recordings. Diastolic filling was classified as normal if the ratio of early to late peak transmitral flow velocity was 1.0 to 2.0 and the deceleration time was 0.14 to 0.23 seconds.[5,6] The Valsalva maneuver was used whenever a normal ratio of early to late peak transmitral flow velocity was obtained, to unmask a possible pseudonormal filling pattern.

Magnetic resonance imaging: All MRI studies were performed in the supine position in a 1.5-T MRI scanner (Siemens Vision, Erlangen, Germany) using a phased-array surface coil. Three scout scans were obtained to define the long and short axes of the left ventricle. Cine turbo fast low-angle shot magnetic resonance images were obtained without tagging in 8 or 9 short-axis slices that were equally spaced from apex to base and in 3 long-axis slices at equal angular intervals around the central axis of the left ventricle (scan parameters were slice thickness 8 mm, in-plane resolution ~1 mm/pixel, temporal resolution 30 to 50 ms depending on heart rate, and echo time/repetition time 4.0/9.0 ms). Control subjects and patients undertook approximately 15-second breath-holds during the scans to eliminate respiratory motion artifacts. View sharing was used to reconstruct 13 to 27 time frames per cardiac cycle, depending on heart rate. Tagged images were then acquired at the same locations as the untagged images (scan parameters were slice thickness 8 mm, in-plane resolution ~1 mm/pixel, temporal resolution 35 or 45 ms depending on heart rate, and echo time/repetition time 4.0/8.9 ms). A segmented k-space version of the spatial modulation of magnetization tagging sequence was used to create a tag grid on the images, with a spacing of 8 mm and width of ~1 mm, immediately after the R-wave trigger. View sharing was used to reconstruct 11 to 23 time frames per cardiac cycle, depending on the heart rate. All images were prospectively gated; therefore, images could not be acquired during the last 10% to 15% of the cycle to allow for detection of the next R-wave trigger. Tags could be visualized and tracked throughout the imaged portion of the cardiac cycle. Tagged magnetic resonance images from a typical patient who had DM are shown in Figure 1.

Images were stored digitally and analyzed offline. Interactive 3-D guide-point modeling[7] was used to define 3-D LV geometry on the untagged images, and mass and volumes were calculated by numerical integration. The motion of the mitral valve annulus plane was tracked by placing guide points at the site of attachment of the mitral valve leaflets to the wall (at the confluence of the left atrium and the left ventricle) on the 3 untagged long-axis images.

Displacement of tagged myocardial points were reconstructed in 3 dimensions from the tagged MR images by deforming a 3-D finite element mathematical model of the left ventricle to match the tracked displacements of the tag stripes.[8] The model interpolated displacement constraints between the tag and image planes, resulting in a consistent 3-D displacement field that was corrected for through-plane motion. The model was then interrogated with standard continuum mechanics methods[9] to provide average measures of circumferential and longitudinal shortening strains, torsional shear strain, and 3-D principal or maximal shortening strain at each time frame. By convention, end-diastole is 0 ms, and each frame was taken at 35- or 45-ms intervals after end-diastole, depending on temporal resolution.

Mitral valve plane motion: The 3-D positions of all mitral valve attachment points were calculated by using image slice location information (encoded in the DICOM header) and averaged to provide an estimate of the mitral valve centroid at each frame. The 3-D

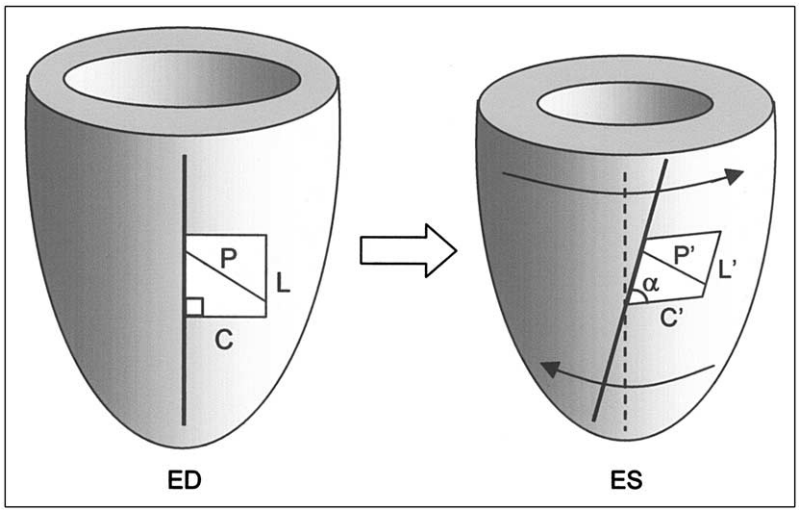

FIGURE 2. Ventricular deformation and myocardial strains. ***(Left)*** **Small line segments in the left ventricle, oriented in the orthogonal circumferential direction at end-systole (C) and longitudinal direction at end-diastole (L).** ***(Right)*** **Systolic deformation of the left ventricle. Thus, circumferential strain is equal to ([C − C′]/C) × 100%, longitudinal strain is equal to ([L − L′]/L) × 100%, and torsional shear strain is equal to 90° − α. Maximal shortening occurs in the direction of the line segment P at end-diastole (ED) (deformed to P′ at end-systole [ES]), so that principal strain is equal to ([P − P′]/P) × 100%. α = angle between C′ and L′; C′ = circumferential direction at end-systole; L′ = longitudinal direction at end-systole.**

displacement of this point was used as the mitral valve plane displacement, and peak systolic and diastolic mitral valve plane velocities were estimated with a 2-point central difference formula.

Myocardial strains: A schematic representation of the myocardial strains examined in this study is provided in Figure 2. Circumferential and longitudinal strains are defined as the percent change in length of small line segments oriented in the circumferential and longitudinal directions, respectively, at end-diastole. Torsional shear strain, a measure of LV "twist" (i.e., rotation of the apex with respect to the base about the central LV axis), is defined as the change in the angle between small material line segments orientated circumferentially and longitudinally at end-diastole.[9] The 3-D principal strain corresponds to the maximal shortening strain developed at any point in the LV myocardium. It is a single 3-D index that combines circumferential and longitudinal axial strains and torsional shear strain and is independent of the coordinate system used to measure these individual components.[9] Increases in circumferential or longitudinal shortening strain or greater LV torsion will each independently lead to an increase in 3-D principal shortening strain. Circumferential and longitudinal strains, torsional angle, and 3-D principal shortening strain were calculated from the Lagrangian strain tensor.[9,10] The 3-D principal shortening strain was calculated as the most negative eigenvalue of the Lagrangian strain tensor.[9] The reported strain measurements represent average values taken over the entire ventricle and are corrected for the effects of through-plane motion. Peak rates of systolic strain and diastolic relaxation of strain were calculated with a central difference formula. The maximum systolic strain rate is given by the peak rate of change of strain measured during systole, and the maximum diastolic strain relaxation rate is given by the peak rate of change of strain measured after peak strain.

Statistical analysis: Data were analyzed with SYSTAT 10.2 (SYSTAT Inc., Evanston, Illinois). All data are presented as mean ± SD. Subject characteristics, echocardiographic measurements, and MRI volumetrics were compared between normal control and diabetes mellitus groups using Student's 2-tailed *t* test. Strain and strain rate depend on age,[10] so comparisons of MRI strains and displacements between patients who had DM and normal subjects were performed with analysis of covariance using age as a covariate. Statistical significance was defined as $p < 0.05$.

RESULTS

Study population: Of 35 patients who had DM and were eligible for MRI, 7 had unacceptable image quality or were intolerant of the procedure (e.g., claustrophobia). Acceptable magnetic resonance images were obtained from all 31 normal control subjects. Characteristics of patients and control subjects are listed in Table 1, and the clinical details of patients who had type 2 DM are presented in Table 2. Patients who had DM had a long history of disease and many had poor metabolic control of the disease. Values for body mass index, heart rate, and diastolic blood pressure were higher for patients than for control subjects. No difference in systolic blood pressure was detected between patients who had DM and control subjects.

Echocardiography: Early diastolic transmitral filling velocity was similar in patients who had DM and control subjects (59 ± 15 cm/s in the DM group vs 59 ± 19 cm/s in the control group, p = NS), but late filling velocity was higher in patients who had DM (68 ± 12 vs 51 ± 14 cm/s, $p < 0.001$). The ratio of early to late peak transmitral flow velocity was lower in patients who had DM (0.9 ± 0.2 vs 1.3 ± 0.6 p = 0.002). None of the patients who had DM had a normal filling pattern.

MRI volumetrics: MRI measurements of LV ejection fraction, end-diastolic volume, end-systolic volume, and stroke volume were comparable in the 2 groups (Table 3). LV mass and the ratio of LV mass to end-diastolic volume were greater in patients who had DM than in control subjects.

Mitral valve plane motion: Figure 3 shows a comparison of mitral valve plane displacement during the cardiac cycle between a typical patient who had DM and a typical control subject. Patients who had DM had a 12% lower peak mitral valve plane displacement (1.1 ± 0.2 vs 1.2 ± 0.3 cm, p = 0.040) than did

TABLE 1 Characteristics of Normal Healthy Control Subjects (NC) and Patients With Type 2 DM

Parameters	NC (n = 31)	DM (n = 28)
Age (yrs)	46.7 ± 23.5	52.6 ± 7.7
Women	10 (32%)	9 (32%)
Body mass index (kg/m^2)	24.5 ± 4.0	32.8 ± 4.9*
Heart rate (beats/min)	70 ± 10	75 ± 9†
Systolic blood pressure (mm Hg)	131 ± 21	134 ± 16
Diastolic blood pressure (mm Hg)	73 ± 14	84 ± 8*

*p <0.001; †p <0.05.
Values are mean ± SD or numbers (percentages).

TABLE 2 Clinical Details of Patients Who Had Type 2 Diabetes Mellitus (n = 28)

Parameters	Value
Smokers	6 (21%)
Controlled hypertension	19 (68%)
Diabetes duration (yrs)	10.5 ± 6.8
Poor glycemic control (hemoglobin A1$_c$ ≥8)	24 (86%)
Hemoglobin A1$_c$ (%)	9.3 ± 1.7
Glucose (mmol/L)	11.0 ± 4.0
Cholesterol (mmol/L)	5.5 ± 0.9
On medication	
Insulin	16 (57%)
β Blockers	3 (11%)
Calcium antagonists	3 (11%)
Angiotensin-converting enzyme inhibitors	18 (64%)
Diuretics	4 (14%)
Cholesterol-lowering drugs	11 (39%)
Antiplatelet agents	6 (21%)

Values are mean ± SD or numbers of patients (percentages).

TABLE 3 MRI Volumetric Data of Normal Healthy Control Subjects (NC) and Patients With Type 2 DM

Parameters	NC (n = 31)	DM (n = 28)
Ejection fraction (%)	70 ± 5	69 ± 7
End-diastolic volume (ml)	126 ± 29	121 ± 33
End-systolic volume (ml)	38 ± 11	38 ± 16
Stroke volume (ml)	88 ± 21	83 ± 22
LV Mass (g)	143 ± 36	200 ± 46*
LV mass/end-diastolic volume (g/ml)	1.2 ± 0.3	1.7 ± 0.3*

*p <0.001.
Values are mean ± SD.

normal subjects. Peak systolic mitral valve plane velocity was not significantly different (4.9 ± 1.3 vs 5.3 ± 1.2, p = NS). However, peak diastolic mitral valve plane velocity was 21% lower in patients who had DM (4.7 ± 1.3 vs 5.9 ± 2.1 cm/s, p = 0.008).

MRI strain: Peak circumferential strain was 14% less (16.7 ± 2.0% vs 19.5 ± 2.4%, p <0.001) and peak longitudinal strain was 22% less (12.5 ± 2.2% vs 16.2 ± 2.1%, p <0.001) in patients who had DM. However, peak torsional shear strain was 17% greater in these patients (6.8° ± 1.4° vs 5.8° ± 1.3°, p = 0.025). Peak principal strain was 10% less in the DM group (24.2 ± 2.4% vs 27.0 ± 2.3%, p <0.001). Figure 3 shows a comparison of temporal evolution of

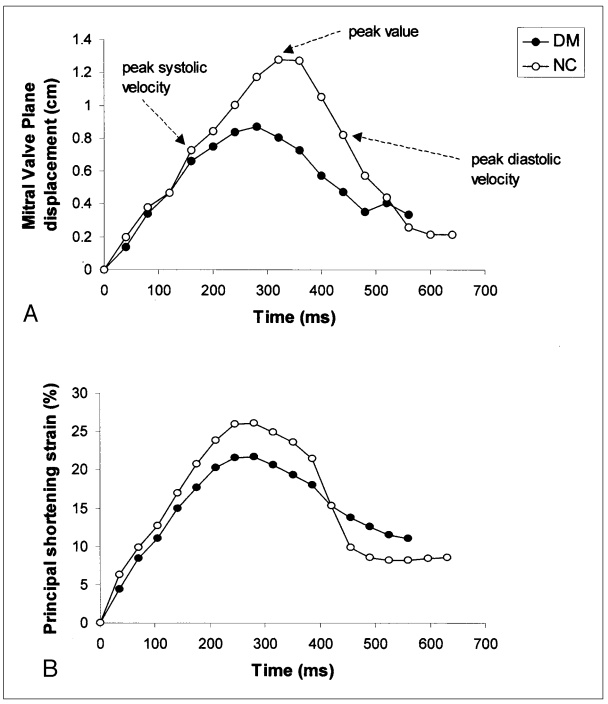

FIGURE 3. Temporal evolution of *(A)* mitral valve plane displacement and *(B)* myocardial principal shortening strain in a typical patient who had type 2 DM compared with a typical normal control (NC) subject. Values were obtained at intervals of 40 ms for mitral valve plane motion and 35 ms for principal shortening strain.

principal shortening strain during the cardiac cycle between a typical patient who had DM and a typical control subject.

During systole, peak circumferential strain rate was 10% lower (88 ± 12% vs 98 ± 11% per second, p = 0.008) and peak longitudinal strain rate was 15% less (69 ± 14% vs 81 ± 11% per second, p = 0.003) in the DM group. Peak rate of change of torsion was 20% greater in the DM group (36° ± 8° vs 30° ± 5° per second, p = 0.002). Peak principal strain rate did not differ significantly between patients and control subjects (117 ± 23% vs 129 ± 22% per second, p = NS).

Peak rate of circumferential strain relaxation was 35% less (71 ± 20% vs 108 ± 41% per second, p <0.001) and peak rate of longitudinal strain relaxation was 32% less (63 ± 21% vs 92 ± 37% per second, p <0.001) in the DM group. Peak rate of relaxation of torsion did not differ between groups (34 ± 11° vs 34 ± 9° per second, p = NS). Peak rate of relaxation of the principal strain was 33% less in the DM group (64 ± 17% vs 96 ± 35% per second, p <0.001).

DISCUSSION

Our results corroborate recent tissue Doppler imaging studies that have shown systolic tissue dysfunction, measured as a decrease in LV longitudinal shortening, in patients who have normal ejection fraction and are assumed to have "isolated" diastolic dysfunction.[11–15] We found that peak LV systolic circumfer-

ential and longitudinal shortening values were lower in the DM group; however, peak LV torsional strain during systole was greater. Thus, peak principal shortening strain, although less in the DM group, was not decreased to as great an extent as the circumferential and longitudinal shortening strains because these decreases were partly compensated for by the increase in peak torsion.

As expected, diastolic relaxation rates of circumferential and longitudinal strains and diastolic mitral valve plane velocity were also lower in patients who had type 2 DM. It is perhaps not surprising that systolic and diastolic indexes of tissue function were impaired because the processes of systole and diastole are interdependent. These results are consistent with those of Yu et al,[16] who found that systolic and diastolic dysfunctions can occur concomitantly with a range of severity in the progression to heart failure.

LV hypertrophy and hypertension commonly coexist in patients who have type 2 DM. A large proportion of our DM group was being treated for hypertension, and increased blood pressure and ratio of LV mass to end-diastolic volume may have influenced the systolic and diastolic strains measured in this study. Fang et al[12] used tissue Doppler imaging to show that myocardial changes due to diabetes are similar to changes caused by LV hypertrophy but are independent and incremental to the effects of LV hypertrophy.[12]

Our results show that the relative diastolic impairment of LV myocardial function was greater than the systolic impairment in the DM group. The diagnostic and prognostic significances of this observation are unknown. Indexes of diastolic function may be more sensitive to pathologic change, but this does not necessarily indicate that diastolic function is impaired sooner than systolic function, as has been suggested by others.[17–19] Therefore, the question of which measurements of strain and strain rate are clinically meaningful must be addressed. Our study implies that the limited tissue strain information obtainable by tissue Doppler imaging in isolated regions of the heart extends to multidimensional strain measurements averaged over the entire left ventricle.

We cannot exclude the possibility of subclinical coronary artery disease in our patients, because coronary angiography was not performed. Therefore, the contribution of undetected cardiovascular disease to impairment of myocardial function in these patients remains unknown. MRI with tissue tagging has lower temporal resolution than tissue Doppler imaging and strain rate echocardiography. However, unlike tissue Doppler imaging, MRI with tagging can provide true estimates of tissue displacement, strain, and strain rate in 3 dimensions. Faster acquisition and analysis methods may allow this technique to be used routinely in clinical practice.[20]

Acknowledgment: The investigators thank Garth Cooper, DPhil, and John Baker, MBChB, of the University of Auckland School of Biological Sciences for help with the recruitment of patients who had diabetes.

1. Mandinov L, Eberli FR, Seiler C, Hess OM. Diastolic heart failure. *Cardiovasc Res* 2000;45:813–825.
2. Sohn DW, Chung WY, Chai IH, Zo JH, Lee MM, Park YB, Choi YS, Lee YW. Mitral annulus velocity in the noninvasive estimation of left ventricular peak dP/dt. *Am J Cardiol* 2001;87:933–936.
3. World Medical Association Declaration of Helsinki. Recommendations guiding physicians in biomedical research involving human subjects. *Cardiovasc Res* 1997;35:2–3.
4. Gardin JM, Dabestani A, Takenaka K, Rohan MK, Knoll M, Russell D, Henry WL. Effect of imaging view and sample volume location on evaluation of mitral flow velocity by pulsed Doppler echocardiography. *Am J Cardiol* 1986;57:1335–1339.
5. Giannuzzi P, Temporelli PL, Bosimini E, Silva P, Imparato A, Corra U, Galli M, Giordano A. Independent and incremental prognostic value of Doppler-derived mitral deceleration time of early filling in both symptomatic and asymptomatic patients with left ventricular dysfunction. *J Am Coll Cardiol* 1996;28:383–390.
6. Xie GY, Berk MR, Smith MD, Gurley JC, DeMaria AN. Prognostic value of Doppler transmitral flow patterns in patients with congestive heart failure. *J Am Coll Cardiol* 1994;24:132–139.
7. Young AA, Cowan BR, Thrupp SF, Hedley WJ, Dell'Italia LJ. Left ventricular mass and volume: fast calculation with guide-point modeling on MR images. *Radiology* 2000;216:597–602.
8. Young AA, Kraitchman DL, Dougherty L, Axel L. Tracking and finite element analysis of stripe deformation in magnetic resonance tagging. *IEEE Trans Med Imaging* 1995;14:413–421.
9. Fung YC. Foundations of Solid Mechanics. Englewood Cliffs, NJ: Prentice-Hall, Inc., 1965:525.
10. Fonseca CG, Oxenham HC, Cowan BR, Occleshaw CJ, Young AA. Aging alters patterns of regional nonuniformity in LV strain relaxation: a 3-D MR tissue tagging study. *Am J Physiol Heart Circ Physiol* 2003;285:H621–H630.
11. Yip GW, Zhang Y, Tan PY, Wang M, Ho PY, Brodin LA, Sanderson JE. Left ventricular long-axis changes in early diastole and systole: impact of systolic function on diastole. *Clin Sci (Lond)* 2002;102:515–522.
12. Fang ZY, Yuda S, Anderson V, Short L, Case C, Marwick TH. Echocardiographic detection of early diabetic myocardial disease. *J Am Coll Cardiol* 2003;41:611–617.
13. Vinereanu D, Nicolaides E, Tweddel AC, Madler CF, Holst B, Boden LE, Cinteza M, Rees AE, Fraser AG. Subclinical left ventricular dysfunction in asymptomatic patients with type 2 diabetes mellitus, related to serum lipids and glycated haemoglobin. *Clin Sci (Lond)* 2003;105:591–599.
14. Petrie MC, Caruana L, Berry C, McMurray JJ. "Diastolic heart failure" or heart failure caused by subtle left ventricular systolic dysfunction? *Heart* 2002;87:29–31.
15. Andersen NH, Poulsen SH, Eiskjaer H, Poulsen PL, Mogensen CE. Decreased left ventricular longitudinal contraction in normotensive and normoalbuminuric patients with type II diabetes mellitus: a Doppler tissue tracking and strain rate echocardiography study. *Clin Sci (Lond)* 2003;105:59–66.
16. Yu CM, Lin H, Yang H, Kong SL, Zhang Q, Lee SW. Progression of systolic abnormalities in patients with "isolated" diastolic heart failure and diastolic dysfunction. *Circulation* 2002;105:1195–1201.
17. Poirier P, Bogaty P, Garneau C, Marois L, Dumesnil JG. Diastolic dysfunction in normotensive men with well-controlled type 2 diabetes: importance of maneuvers in echocardiographic screening for preclinical diabetic cardiomyopathy. *Diabetes Care* 2001;24:5–10.
18. Raev DC. Which left ventricular function is impaired earlier in the evolution of diabetic cardiomyopathy? An echocardiographic study of young type I diabetic patients. *Diabetes Care* 1994;17:633–639.
19. Schannwell CM, Schneppenheim M, Perings S, Plehn G, Strauer BE. Left ventricular diastolic dysfunction as an early manifestation of diabetic cardiomyopathy. *Cardiology* 2002;98:33–39.
20. Sampath S, Derbyshire JA, Atalar E, Osman NF, Prince JL. Real-time imaging of two-dimensional cardiac strain using a harmonic phase magnetic resonance imaging (HARP-MRI) pulse sequence. *Magn Reson Med* 2003;50:154–163.